

L17ER4: A cell-permeable attenuated cationic amphiphilic lytic peptide

Kenta Shinga,[§] Takahiro Iwata,[§] Kazuya Murata,[‡] Yoko Daitoku,[‡] Junya Michibata,[§] Jan Vincent V. Arafiles,[§] Kentarou Sakamoto,[§] Misao Akishiba,[§] Tomoka Takatani-Nakase,^{#,¶} Seiya Mizuno,[‡] Fumihiro Sugiyama,[‡] Miki Imanishi,[§] Shiroh Futaki^{§*}

[§]Institute for Chemical Research
Kyoto University
Gokasho, Uji, Kyoto 611-0011, Japan

[‡]Laboratory Animal Resource Center, Transborder Medical Research Center, Faculty of Medicine, University of Tsukuba
Tennodai 1-1-1, Tsukuba, Ibaraki 305-8575, Japan

[#]School of Pharmacy and Pharmaceutical Sciences, Mukogawa Women's University, Nishinomiya, Hyogo 663-8179, Japan

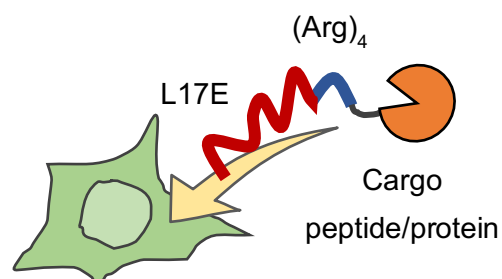
[¶]Institute for Bioscience, Mukogawa Women's University, Nishinomiya, Hyogo 663-8179, Japan

*Corresponding author
Shiroh Futaki
Institute for Chemical Research
Kyoto University
Gokasho, Uji, Kyoto 611-0011, Japan
E-mail: futaki@scl.kyoto-u.ac.jp

Abstract

We have developed a series of attenuated cationic amphiphilic lytic (ACAL) peptides that can efficiently bring immunoglobulin G (IgG) and other functional proteins into cells. Delivery is generally achieved through the coadministration of ACAL peptides with cargo proteins. However, conjugation of ACAL peptides with cargos may be a promising approach for *in vivo* application to link *in vivo* outcomes of ACAL peptides and cargos. This study describes the creation of a new cell-permeable ACAL peptide, L17ER4. L17E is an optimized prototype of ACAL peptides previously developed in our laboratory for efficient delivery of IgGs into cells. Delivery was improved by functionalizing L17E with a tetra-arginine (R4) tag. Compared to the use of R8, a representative cell-penetrating peptide with high intracellular delivery efficacy, conjugation with L17ER4 afforded approximately four-fold higher cellular uptake of model small-molecule cargos (fluorescein isothiocyanate and HiBiT peptide). L17ER4 was also able to deliver proteins to cells. Fused with L17ER4, Cre recombinase was delivered into cells. Intracerebroventricular injection of Cre-L17ER4 into green red reporter mice, R26GRR, led to significant *in vivo* gene recombination in ependymal cells, suggesting that L17ER4 may be used as a cell-penetrating peptide for delivering protein therapeutics into cells *in vivo*.

Graphical abstract



Keywords

Attenuated cationic amphiphilic lytic (ACAL) peptide; oligoarginine; cell-penetrating peptide; intracellular protein delivery; Cre recombinase

Introduction

Considerable research interest has been focused on the development of ways to deliver bioactive peptides and proteins into cells.¹⁻³ Cell-penetrating peptides (CPPs) are among the most promising means to achieve such delivery.⁴⁻⁷ Conjugation or complexation of a protein or peptide of interest with CPPs can confer membrane permeability. Arginine-rich peptides derived from the HIV-1 Tat protein and oligoarginines are widely used CPPs.⁸⁻¹¹ In addition, CPPs with secondary and primary amphiphilic structures (e.g., penetratin and TP-10, respectively) have been developed.^{12, 13}

The internalization routes of these CPPs and conjugates include direct penetration through the plasma membrane.^{14, 15} However, in most cases, endocytosis is the dominant route, especially for conjugated proteins of high molecular weight. After endocytic uptake, some fractions of CPPs and their conjugates are thought to be released through endosomal membranes to reach the cytosol (i.e., endosomal escape) and thus exert their expected effect in cells. However, the efficiency of endosomal escape by CPPs is generally unsatisfactory, and there is still room for improvement in efficacy.¹⁶

One potential approach to improve the efficacy of endosomal escape of CPPs is to form a conjugate with peptides and other chemical species that can rupture endosomal membranes. Peptides possessing this ability (i.e., endosomolytic peptides) generally have an amphiphilic structure, leading to rupture of membranes to allow the leakage of endocytosed materials into the cytosol.¹⁷ Perturbation of the cell membrane should allow leakage of cellular components to outside cells, accompanied by damage to cells. Therefore, preferential perturbation of endosomal membranes over the cell membrane is required.

One of the most popular approaches to gain this functionality is to utilize the pH difference between the cell surface and endosomal interior. A decrease in pH accompanies endosomal maturation and reaches mildly acidic level (approximately pH 5), whereas the condition outside cells is considered to be almost neutral (about pH 7).⁷ Accordingly, various pH-sensitive peptides have been designed to exploit this pH difference.¹⁸⁻²¹ Many of these methods have been employed for gene/nucleic acid delivery often with satisfactory results. However, higher efficiency is often required for intracellular protein delivery.

We have designed a series of peptides, intended to exhibit effective entrapment by endosomes followed by membrane lysis at the decreased endosomal pH.²²⁻²⁸ Cationic amphiphilic peptides generally have potent membrane lysis activity while the placement of glutamate (negatively charged at neutral pH) in the hydrophobic face of the amphiphilic peptides should lead to a decrease in membrane rupture tendency against cell

membranes. Such peptides are collectively termed attenuated cationic amphiphilic lytic (ACAL) peptides.⁵ When the peptides are delivered in endosomes, the decrease in pH can lead to protonation of glutamate. The accompanying increase in the net hydrophobicity of the peptides then leads to an increase in the membrane perturbation ability and subsequent membrane rupture. The cell surface presents a weak negative charge. Limiting the number of glutamate insertions in the hydrophobic face and their retention of a net positive charge, favors cell surface accumulation which in turn favors endocytosis into endosomes. Pronounced cytosolic delivery of bioactive proteins, including immunoglobulin G (IgG), was achieved in the presence of these peptides. However, chemical conjugation of the ACAL peptides with proteins to be delivered into cells (i.e., cargos) can actually yield poorer results than their mixing together.²⁷ The relatively high hydrophobicity of ACAL peptides and the resulting rupture of the membrane allow cargo to translocate into the cytosol when a mixture of cargos and ACAL peptides are administered to cells. However, once conjugated, although the membranes are perturbed, the cargo is anchored with ACAL peptides attached to membranes and thus may not be effectively liberated into the cytosol. On the contrary, when *in vivo* application of ACAL peptides is intended, conjugation of the ACAL peptides and cargos is a practical approach. These peptides should be peripheral to the target cells for cargo delivery. Due to their potential difference in pharmacokinetics and *in vivo* fate, optimal *in vivo* delivery cannot usually be achieved without conjugation or packaging into vehicles such as lipidic or polymer nanoparticles.

In this study, the efficacy of the intracellular delivery of peptides and proteins conjugated with L17E and its derivatives was evaluated. Although L17E was not very effective in this type of application, an L17E analog tagged with four arginine residues at the C-terminus (L17ER4) was found to be effective, showing comparable or higher delivery activity when tagged with octaarginine (R8), a representative CPP.^{29, 30} The efficacy of L17ER4 was exemplified in the delivery of HiBiT peptide (an 11-residue peptide to form a complex with ~18 kDa LgBiT protein segment for split luciferase assay) and Cre recombinase (38 kDa) into HeLa cells. Cerebral ventricle injection of a Cre recombinase fusion protein with L17R4 (Cre-L17ER4) led to Cre/loxP recombination in Cre-reporter knock-in mice, suggesting the potential of L17R4 for *in vivo* delivery.

Material and Methods

Materials

Fmoc-protected amino acids and coupling agents were purchased from Peptide Institute, Watanabe Chemical Industries, and Novabiochem. Other reagents, including salts and incubation media, were obtained from Sigma-Aldrich, FUJIFILM Wako Chemicals, and Thermo Fischer Scientific unless otherwise specified. Peptides were dissolved in dimethylsulfoxide (DMSO) to yield a final DMSO concentration (1%) when diluted in the culture media.

Peptide synthesis

All the peptides used in this study were synthesized on a Shimadzu PSSM-8 peptide synthesizer using Fmoc (=9-fluorenylmethyloxycarbonyl)-solid-phase peptide chemistry with TGS-RAM resin (Shimadzu) as reported previously.³¹ A coupling system using 2-(1*H*-Benzotriazole-1-yl)-1,1,3,3-tetramethyluronium hexafluorophosphate (HBTU)/1-hydroxybenzotriazole (HOBt)/*N,N*-diisopropylethylamine (DIEA) was employed. After synthesis, deprotection of the protecting groups and detachment of peptides from the resin were performed using trifluoroacetic acid (TFA)/1,2-ethanedithiol (EDT) (95:5) at 23 °C for 3 h followed by purification via reverse-phase high-performance liquid chromatography (RP-HPLC). FITC (=fluorescein isothiocyanate)-labeled peptides were prepared as reported, by the selective on-resin modification of lysine with FITC using the Mtt (=methyltrityl) group as the side chain protecting group.³² The masses of the obtained peptides were confirmed by matrix-assisted laser desorption ionization time-of-flight mass spectrometry (MALDI-TOFMS) (Table S1).

Cell Culture

HeLa cells (human epithelial carcinoma cell line) obtained from The European Collection of Authenticated Cell Cultures (ECACC) (93021013) were cultured in α -minimum essential medium (α -MEM) supplemented with 10% (v/v) heat-inactivated bovine serum (BS) (α -MEM(+)). The cells were maintained at 37 °C, in a humidified 5% CO₂ incubator, and subculture was conducted every 3-4 days.

*WST-8 assay*³³

Cell viability was determined using Cell Counting Kit-8 (CCK8) (Dojindo), following the manufacturer's protocol. Briefly, HeLa cells were treated with peptides for 1 h in serum-free α -MEM (α -MEM(-)). WST-8 was then added, and the cells incubated for another 2 h.

Confocal laser scanning microscopy (CLSM) analysis of FITC-labeled peptides

HeLa cells were seeded in 35 mm glass-bottom dishes (Iwaki) and were cultured at 37 °C, with 5% CO₂ for 24 h until 80-90% confluence. Cells were washed twice with phosphate-buffered saline (PBS) and were then incubated with FITC-labeled peptides in α -MEM(-) or α -MEM(+) for 1 h at 37 °C. For the 4°C experiment, cells were pre-incubated at 4 °C for 30 min. Cells were then washed with cold PBS and incubated in the presence of L17ER4(FITC) (3 μ M, α -MEM(+)) for 1 h at 4 °C. For the time course experiment, Cells were washed twice with PBS and were then incubated with FITC-labeled peptides in α -MEM(-) or α -MEM(+) for 5, 20, 40, and 60 min at 37°C, respectively. After washing 4 times with PBS containing 0.5 mg/mL heparin sodium, α -MEM(+) was added on dishes and cellular localization of FITC-labeled peptides was analyzed via live-cell imaging using FV3000 Olympus confocal laser scanning microscopy (CLSM).

Flow cytometric analysis of FITC-labeled peptides

HeLa cells were seeded in 24-well plate (Iwaki), and cultured at 37 °C with 5% CO₂ for 24 h until 80-90% confluence. Cells were washed twice with PBS and were then incubated with FITC-labeled peptides in α -MEM(+) for 1 h at 37 °C. For the 4°C experiment, cells were pre-incubated at 4 °C for 30 min. Cells were then washed with cold PBS and incubated in the presence of L17ER4(FITC) (3 μ M, α -MEM(+)) for 1 h at 4 °C. For the time course experiment, cells were washed twice with PBS and were then incubated with FITC-labeled peptides in α -MEM(-) or α -MEM(+) for 5, 10, 15, 30, 45, and 60 min at 37 °C, respectively. After washing 4 times with PBS containing 0.5 mg/mL heparin sodium, cells were dislodged using 0.01% trypsin, transferred to microcentrifuge tubes, and centrifuged (800 \times g, 5 min, 4 °C). The supernatant was discarded. The pellet was washed with PBS containing 0.5 mg/mL heparin sodium. The resulting pellet was resuspended in 500 μ L PBS containing 0.5 mg/mL heparin sodium, followed by flow cytometric analysis of 10,000 gated events using Attune NxT (Thermo Fisher Scientific).

*HiBiT/LgBiT recombination assay*³⁴

HeLa cells (1.0×10^4 cells) were seeded into 96 well microplates (Iwaki). The cells were washed with PBS(-) twice and transfected with LgBiT Expression Vector (Promega) using Lipofectamine LTX reagent (Invitrogen) following manufacturer's protocol for 24 h. After incubation, cells were washed twice with PBS(-) and incubated with 2.5 μ M HiBiT peptides in α -MEM(+) for 30 min at 37 °C. After removing the media, Nano-Glo live cell assay reagent (Promega) was added, and the luminescence was analyzed by

GloMax Navigator Microplate Luminometer (Promega).

Preparation of peptide-fused Cre proteins

An *E. coli* expression vector, Cre-His6-pET42b, was constructed by inserting DNA fragment encoding Cre-Myc sequences amplified from pCAG-Cre (plasmid 13775, Addgene) by PCR into NdeI/EcoRI sites of pET42b(+). CreL17E-His6-pET42b and CreL17ER4-His6-pET42b plasmids were constructed by inserting DNA fragments encoding L17E and L17ER4 into BglIII/EcoRI sites of Cre-His6-pET42b, respectively. *E. coli* BL21(DE3) cells transformed with one of these expression vectors were incubated in LB medium at 37°C, added 0.1 mM IPTG at OD₆₀₀ = ~0.6, and further incubated overnight at 18°C. The soluble fraction was purified by the HisTrapFF column (GE Healthcare) using binding buffer (50 mM Tris-HCl, 500 mM NaCl, 25 mM imidazole, pH 7.4) and elution buffer (50 mM Tris-HCl, 500 mM NaCl, 250 mM imidazole, pH 7.4). The eluted proteins were concentrated, and buffer was exchanged by Amicon Ultra 10K centrifugal filter devices (Merck) using PBS(-) with 400 mM NaCl.

*Cre/loxP recombination assay*³⁵

LoxP-DsRed-loxP-EGFP-N1 plasmid (loxP-reporter plasmid) and Cre protein were prepared as previously reported.²⁵ LoxP reporter was transfected into HeLa cells using Lipofectamine LTX following manufacturer's protocol for 24 h. After incubation, cells were washed twice with PBS(-) and were incubated with 5 or 10 μM Cre protein in the presence of a peptide in α-MEM(-) for 1 h at 37 °C. Cells were then washed twice PBS(-) and incubated in α-MEM(+) for 24 h at 37 °C. After washing twice with PBS(-), α-MEM(+) were added on dishes and cells were imaged using CLSM.

Cre/loxP recombination assay at the lateral ventricle of Cre-reporter knock-in mice

All mouse experiments were performed under the approval of institutional animal care and use committee in the University of Tsukuba. ROSA26 Cre-reporter knock-in C57BL/6N mice (R26GRR mice, adult male)³⁶ were used in this experiment. Under anesthesia, Cre and peptide-fused Cre (40 μM in 5 μL) were injected into the right lateral ventricle and fed for seven days. The mice were then sacrificed by perfusion fixation under anesthesia with phosphate-buffered saline, followed by 4% paraformaldehyde. The olfactory bulbs and cerebellums were excised from the harvested brains. Fluorescent images of the posterior cut surface were obtained using a model M165 FC fluorescence stereomicroscope (Leica) and a VB-7010 cooled CCD color camera (Keyence). After equilibration with 10%, 20%, and 30% sucrose, the brains were embedded to O.C.T.

compound and sliced frozen brain tissue (10 μm) was acquired. The nuclei were stained with Hoechst 33258 and the fluorescence of tDsRed (a tandem version of dimeric DsRed) and Hoechst were detected using a model BZ-X710 fluorescence microscope (Keyence).

Results and discussion

Peptide design

To analyze the intracellular fate of L17E, fluorescein isothiocyanate (FITC)-labeled L17E was prepared. FITC also serves as a model small molecule to be delivered into cells. Considering that N-terminal interaction with membranes is often important for amphiphilic peptides,³⁷ and that L17E also has a potential amphiphilic structure, a glyceryl lysine segment was added at the C-terminus of L17E and FITC was added to the ϵ -amino moiety of the lysine side chain.

L17E was effective in transiently perturbing membranes to allow extracellular cargo molecules to translocate into the cytosol. On the contrary, the relatively high hydrophobicity of L17E may lead to the peptide being retained by the membranes, hampering their cytosolic distribution. One promising idea to release the peptide from membranes is to increase the net hydrophilicity while retaining the membrane perturbation ability of L17E. To this end, a series of L17E analogs having two or four residues of arginine via a glycine spacer at the N- or C-terminal side of the peptide were designed [L17ER2(FITC), L17ER4(FITC), R2L17E(FITC), and R4L17E(FITC)] (Figure 1A). The addition of arginine residues may increase the net hydrophilicity of the peptides, while gently interacting with cell surface molecules via hydrogen bond formation and electrostatic interactions – it is known that arginine-rich peptides are often membrane permeable and are generally more capable than lysine-rich peptides.¹¹ The addition of arginine residues may thus favorably work for cell surface adsorption and endocytic uptake of peptides, and eventual cytosolic release of peptides after their translocation through endosomal membranes.

The peptide chain was prepared using conventional Fmoc (=9-fluorenylmethyloxycarbonyl)-based solid-phase peptide synthesis, where Lys(Mtt) (Mtt=4-methyltrityl) derivative was incorporated at the lysine for FITC-labeling. After completion of peptide chain construction, N-terminus of the protected peptide on resin was blocked by Boc (=tert-butoxycarbonyl) group, the Mtt group on the lysine was selectively removed by the treatment with hexafluoroisopropanol and dichloromethane (1:4 v/v),³² and the liberated ϵ -amino acid was labeled with FITC. Final deprotection and detachment from the resin using trifluoroacetic acid (TFA) in the presence of 1,2-ethanedithiol (EDT) (95:5), followed by high-performance liquid chromatography (HPLC) purification yielded the desired peptide. The molecular weight of the product was confirmed by matrix-assisted laser desorption/ionization mass spectrometry (MALDI-TOFMS) (Table S1).

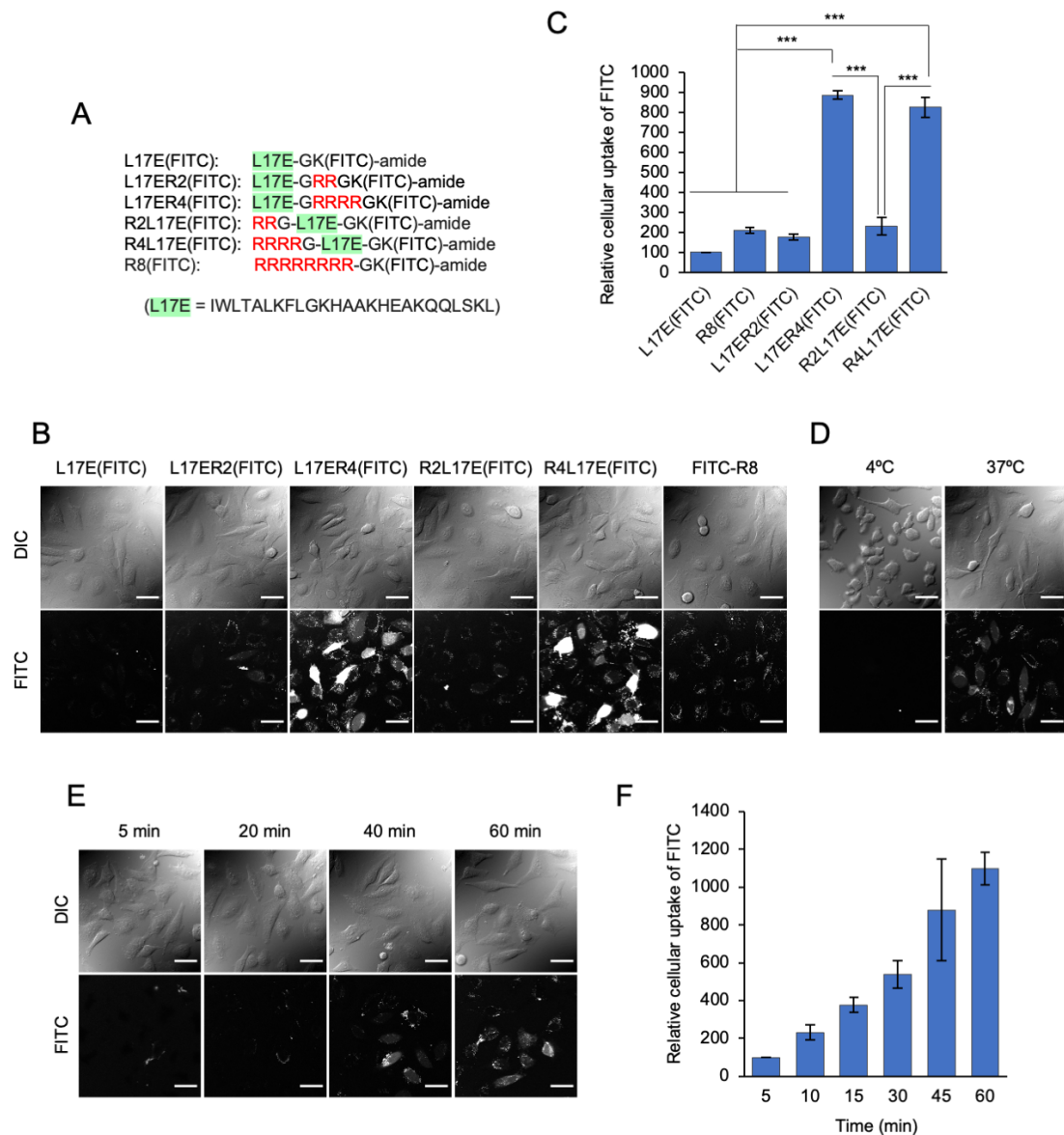


Figure 1. (A) L17E and its analogs conjugated with a model small-molecule cargo, FITC. (B) Confocal scanning microscopy analysis of the cells treated with L17E (FITC) and the related peptides (6 μ M each) for 1 h in serum-containing medium. Upper and lower panels represent differential interference contrast (DIC) and fluorescence images, respectively. (C) Flow cytometry analysis of total cellular uptake of FITC after incubation with 6 μ M peptides for 1 h in serum-containing medium. Results are presented as mean \pm standard error of mean (SEM) ($n = 3$). ***: $p < 0.0001$. Tukey-Kramer's honestly significant difference test. (D) CLSM images of cells treated with 3 μ M L17ER4 (FITC) for 1 h at 4°C. (E) Time-course observation of cells treated with 3 μ M L17ER4 (FITC) and (F) total cellular uptake. Results are presented as the mean \pm SEM ($n = 3$). Scale bars, 40 μ m.

Cellular uptake of L17E and the analogues

Prior to analysis of cellular uptake of L17E (FITC) and its analogs, the cytotoxicity of these peptides after incubation for 1 h in serum-containing medium was analyzed by WST-8 assay³³ (a mitochondrial dehydrogenase activity-based assay, suggesting no serious cytotoxicity at a peptide concentration of 6 μ M or less (Figure S1)). HeLa cells were treated with L17E(FITC) and its analogs (6 μ M) for 1 h, and the cellular distribution was analyzed by confocal laser scanning microscopy (CLSM) (Figure 1B). FITC-labeled octaarginine (FITC-R8),¹¹ a representative CPP, was used as a positive control. Cells treated with 6 μ M FITC-R8 yielded dot-like or punctate FITC signals in cells, suggesting that the peptide was taken up into cells by endocytosis and a considerable fraction of the peptide was retained in endosomes. Cells treated with L17E(FITC) yielded signals that were hardly detectable under the same microscopy setting, suggestive of lower levels of cellular uptake. Punctate signals were observed in cells treated with L17ER2(FITC) and R2L17E(FITC). By contrast, strong FITC signals were observed in cells treated with L17ER4(FITC) and R4L17E(FITC). The diffuse appearance of fluorescence signals throughout the cells, in addition to the dot-like signals, were suggestive of cytosolic translocation of these peptides. Flow cytometry analysis of cellular uptake of these peptides also suggested that L17ER4 and R4L17E yielded 4.3-fold greater intracellular FITC signal than other L17E analogs and R8 (Figure 1C), presumably due to the adequate balance of hydrophobicity and hydrophilicity needed for effective membrane interaction and translocation of the peptides. Although L17ER4 and R4L17E seem to have comparable cellular uptake efficacy in flow cytometry analysis, the former peptide yielded more cytosol-localized fluorescence signals and was thus employed for further study.

The involvement of endocytosis in the cellular uptake of L17ER4 was confirmed by the significant loss of L17ER4(FITC) uptake by cells held at 4°C for 1 h (Figure 1D). Endocytosis is an energy-driven cellular process that does not occur with high efficiency at 4°C as ATP is not generated efficiently. In contrast to the treatment at 37°C, no significant signals were observed in cells treated with L17ER4(FITC) at 4°C. A time-course study of the cells treated with L17ER4(FITC) also suggested the involvement of endocytosis (Figure 1E). No substantive FITC signals were observed in cells 5 min after the addition of L17ER4(FITC) to the cell culture media. Dot-like signals became apparent at 20 min, and diffuse cytosolic signals were observed after 40 min. Flow cytometry analysis showed a time-dependent increase in total cellular uptake of FITC (Figure 1F). These results confirm the potential of L17ER4 as an intracellular delivery peptide.

Intracellular delivery of the HiBiT peptide

As noted above, FITC can be considered as a model cargo of small molecular weight. Microscopic observation using fluorescently labeled cargo is frequently employed to analyze intracellular delivery efficacy. However, it is often difficult to evaluate cytosolic translocation when a considerable fraction of the cargo is retained in endosomes. In this circumstance, signals from cytosolic localized cargos are rather weak compared with intense signals from endosomes and can only obtain marginal signals that cannot be discriminated from cellular autofluorescence. Therefore, we next evaluated the delivery efficacy of L17E analogs in terms of the activity of the delivered cargo.

HiBiT is an 11-residue peptide developed by Promega, which can form a complex with a large fragment [Large Bit (LgBiT), *ca.* 18 kDa) derived from small luciferase (NanoLuc) with a dissociation constant (K_d) of 700 pM.³⁸ The resulting complex of the split segments, HiBiT with LgBiT, shows luciferase activity. The delivery efficacy of the L17E derivatives was evaluated by delivery of the HiBiT peptide tagged with L17E derivatives into LgBiT-expressing cells (Figure 2A).

The tandem conjugates of L17E and its analogs with HiBiT thus prepared (Figure 2B, 2.5 μ M) were treated with HeLa cells transfected with the LgBiT-expressing plasmid in serum-containing medium for 30 min at 37°C and then luciferase activity was analyzed. R8-HiBiT and N-terminally acetylated HiBiT (2.5 μ M each) were used as controls. We noted that no marked cytotoxicity was observed at the employed peptide concentration of 2.5 μ M (Figure S2). L17ER4 yielded a 5-fold luminescence increase compared to Ac-HiBiT (Figure 2C). R8-HiBiT yielded a 1.6-fold luminescence increase compared with Ac-HiBiT, but only \sim 1/3 that of L17ER4-HiBiT. Considering that R8 has been frequently employed as a representative CPP of high efficacy, the above results suggest the potential of arginine-tagged L17E analogs, especially L17ER4, as an intracellular delivery vector. Additionally, the ability of L17ER2 to deliver HiBiT intracellularly was also evaluated, and was almost comparable to that of R8. Comparison of the results obtained in Figures 1C and 2C suggested that the cellular activity obtained by the cytosolic delivery of small molecules by CPPs is in accordance with the total cellular uptake of cargo molecules.

The original method of L17E to introduce cargo proteins (including antibodies) into cells involves simply adding a mixture of cargo together with a relatively high concentration of L17E (typically 40 μ M), without conjugating them to each other. In this study, the delivery efficacy of HiBiT peptide using the L17ER4 conjugate (2.5 μ M) was compared with simple admixture by incubating 2.5 μ M HiBiT with 40 μ M L17E (Figure 2D). Although co-incubation of 2.5 μ M HiBiT with 40 μ M L17E yielded a higher luminescence than incubation with 2.5 μ M L17ER4-HiBiT, the difference was not

significant. Given the preferable *in vivo* applicability of the L17ER4-HiBiT conjugate, the results shown in Figure 2D do not detract from the feature of L17ER4 as a CPP.

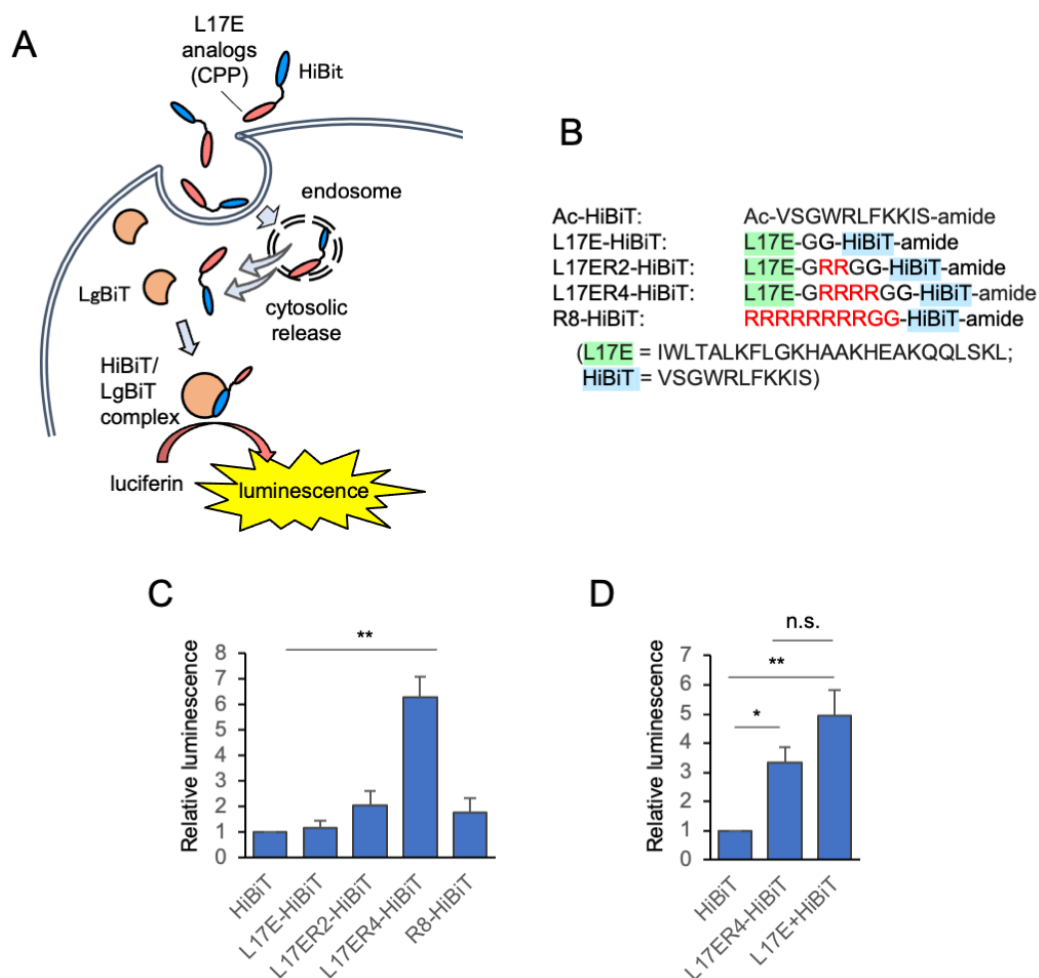


Figure 2. (A) Schematic illustration of evaluation of cytosol delivery ability of CPPs using HiBiT/LgBiT split luciferase system. (B) Sequences of HiBiT peptides conjugated with CPPs. Luminescence obtained by the intracellular delivery using L17ER4-HiBiT in comparison with (C) other CPP-HiBiT conjugates (2.5 μ M each) and (D) a mixture of 2.5 μ M HiBiT and 40 μ M L17E. Results are presented as the mean \pm SEM (n = 3). *: $p < 0.05$, **: $p < 0.001$, n.s.: not significantly different (C, Dunnett's test; D, Tukey-Kramer test).

Intracellular delivery of Cre recombinase

Next, we evaluated the applicability of L17ER4 in protein delivery using Cre recombinase as a cargo. The Cre-loxP recombination assay system was used. Cytosolic delivery of Cre results in gene recombination, and the efficacy of the delivery system can be evaluated based on the extent of recombination.

HeLa cells transiently transfected with the *loxP-DsRed-STOP-loxP-EGFP* reporter plasmid were treated with fusion proteins of Cre with L17E, and L17ER4 (5 μ M each). When Cre was successfully delivered, the DsRed coding region flanked by two loxP sites was removed, allowing the expression of EGFP (Figure 3A). The cells were incubated with Cre fused with peptides for 1 h, followed by replacement with fresh media absent Cre analogs and incubation for 24 h. CLSM analysis suggested that incubation with Cre-L17E resulted in ~10% of the total fluorescent protein-expressing cells (DsRed and EGFP) showing EGFP (Figure 3B, C). Under the same treatment, Cre-L17ER4 yielded ~25% EGFP expression. The efficacy of the 5 μ M Cre-L17ER4 fusion protein was also comparable to that obtained by treatment with 5 μ M Cre in the presence of 40 μ M L17E (a previously reported protocol) (Figure 3D). Therefore, conjugation with L17ER4 successfully reduced the needed concentration of the ACAL peptide compared to free L17E.

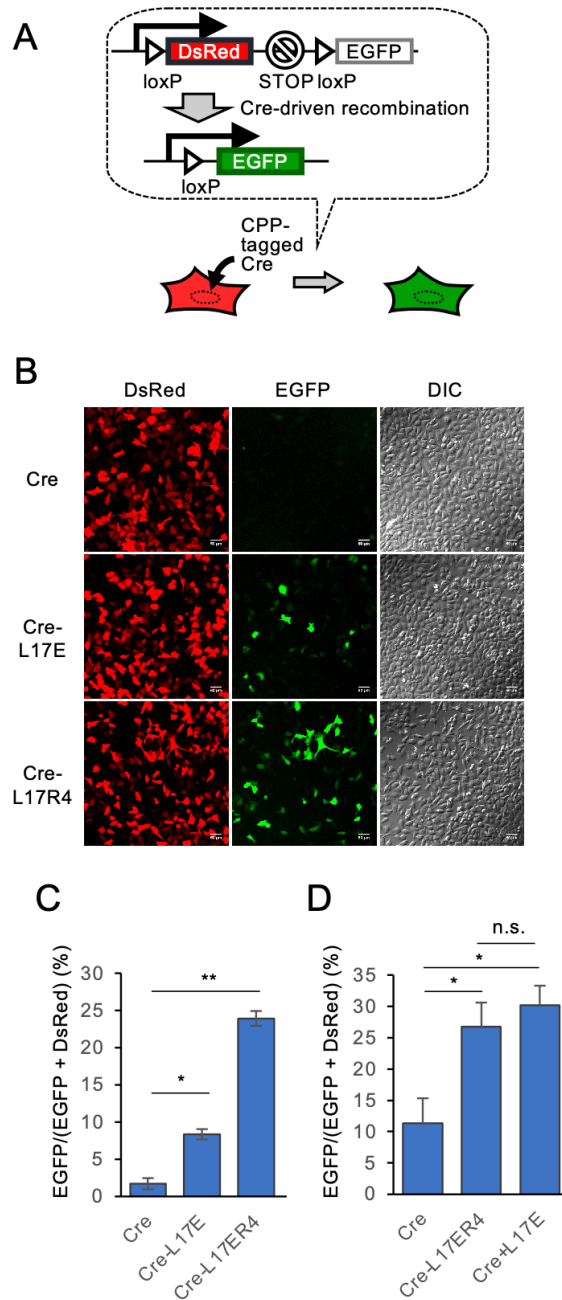


Figure 3. (A) Outline of Cre-loxP recombination assay. (B) CLSM images of loxP-DsRed-loxP reporter cells treated with Cre and the CPP-fused Cre recombinases for 1 h. Scale bars, 50 μ m. Recombination efficiencies expressed as percent of EGFP-expressing cells over the total number of fluorescence-emitting cells (DsRed + EGFP cells) after the treatment of the cells with (C) Cre, Cre-L17E, and Cre-L17ER4 (5 μ M each), and (D) a mixture of 5 μ M Cre and 40 μ M L17E, respectively. *: $p < 0.05$, **: $p < 0.001$, n.s.: not significantly different based on Tukey-Kramer's test.

In vivo application of L17ER4 as a delivery peptide

We next analyzed the potential *in vivo* application of L17ER4 through intracerebroventricular (i.c.v.) administration of Cre-L17E or Cre-L17ER4 into the cerebral ventricle of green red reporter mice (R26GRR). Cellular entry of Cre recombinase leads to an EGFP-to-tDsRed change in fluorescence. Thus, we evaluated the *in vivo* distribution and efficacy of Cre delivery using L17ER4. This assay was also successfully employed previously to assess the potential application of an L17E analog, HAad peptide, for *in vivo* cytosolic delivery.³⁹ The cerebral ventricles are cavities in the brain filled with cerebrospinal fluid and i.c.v. administration is a potential route for drug delivery into the brain.⁴⁰ The cerebral ventricle is comprised of four interconnected ventricles (i.e., right, left, third, and fourth ventricles).

Cre-L17ER4 was injected into the right lateral ventricle of R26GRR mice³⁶ (Figure 4A). Seven days later, the mice were anesthetized and perfused with paraformaldehyde in phosphate-buffered saline (PBS). Brains were then dissected at the coronal section, and sliced frozen brain tissue (10 μm) was acquired (Figure 4B, C).

The cryosection images with Hoechst 33258-stained nuclei (indicating localization of the cells in the brain) close to the injection site showed red signals of tDsRed, suggesting successful gene recombination by the internalization of Cre-L17ER4 (Figure 4C, Cre-L17ER4). Significant recombination was observed in ependymal cells (cells lining the cerebral ventricle) that face the lateral ventricle. No significant tDsRed signals were observed in the brain parenchyma, suggesting the limited accessibility of the current systems to cells located on tissue surfaces. Notably, tDsRed signals were also observed in ependymal cells facing the left lateral ventricle, suggesting that Cre-L17ER4 likely spread into the other lateral ventricle. Cre-L17E and Cre alone also induced tDsRed expression in ependymal cells (Figure 4C, Cre-L17E, Figure S3A, Cre); however, the efficacy was much lower than that attained by Cre-L17ER4.

When the brain was sliced at the posterior and observed from the cerebellum side, the cerebral ventricle is observed in the central part of the brain (i.e., third ventricle) (Figure 4D, E). Fluorescence microscopic analysis of the slice obtained from Cre-L17ER4-treated mice showed red tDsRed signals around the cerebral ventricle, while the whole section had green EGFP signals (Figure 4E, Cre-L17ER4). This also suggested the distribution of Cre-L17ER4 in the cerebral ventricle, entering the cells. Marginal red signals were observed in mice treated with Cre and Cre-L17E, compared with control mice treated only with buffer (Figure 4E and Figure 3SB, Cre-L17E/Cre versus buffer). Additionally, the tendency was comparable to that obtained using the HAad peptide.³⁹

Taken together, the results suggest the potential applicability of L17ER4 for *in vivo*

delivery.

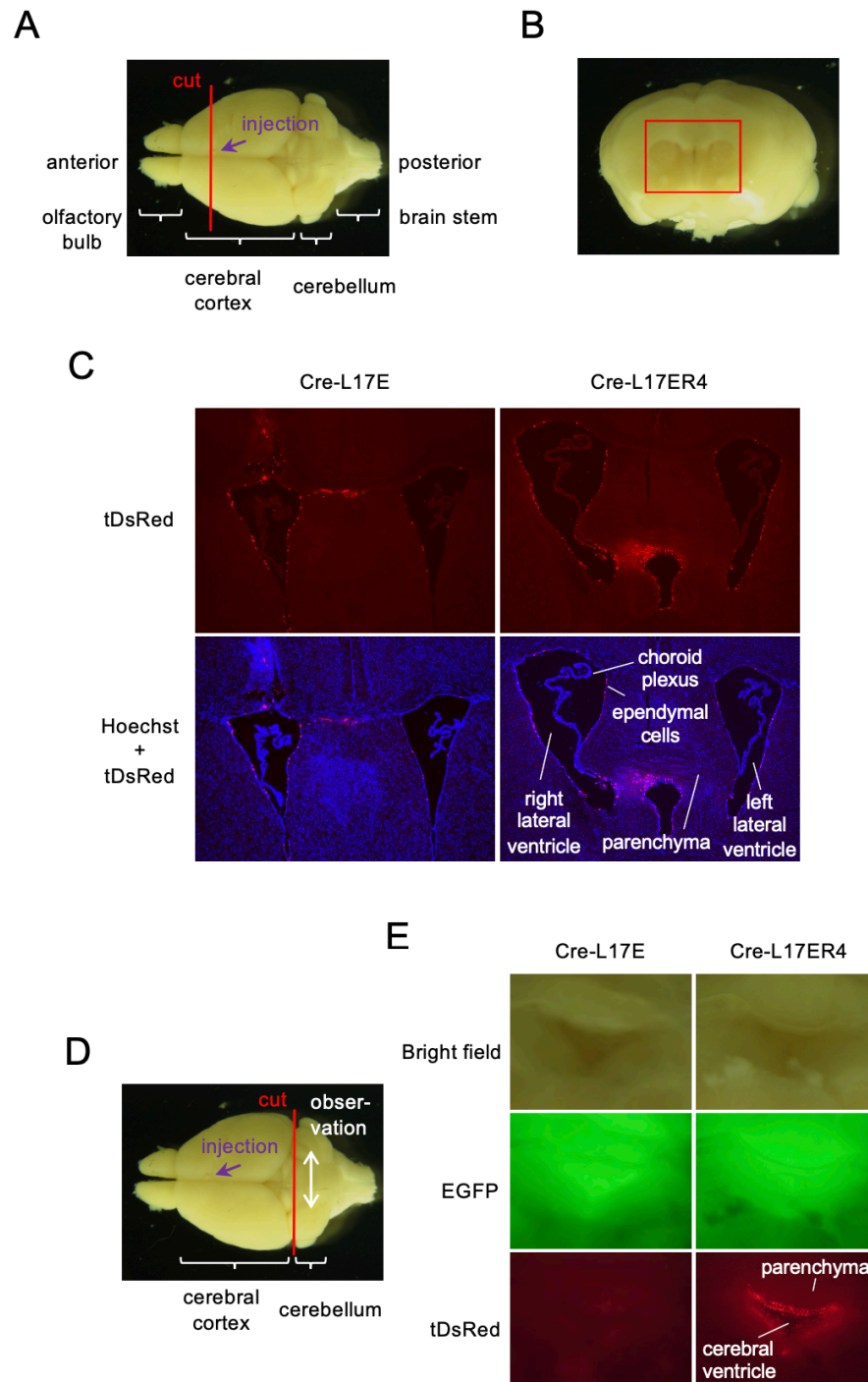


Figure 4. CPP-mediated i.c.v. delivery of Cre recombinase into ependymal cells and choroid plexus faced to the lateral ventricle. (A) Mouse brain and (B) the coronal section of the brain along the red line in (A), observed from the brain anterior. Cre recombinase fused with CPPs (40 μ M in 5 μ L) were injected into the right lateral ventricle. (C) Fluorescence images of the cryosection of the brain close to the injection site (corresponding to the boxed area in (B)). Nuclei were stained with Hoechst 33258 (blue). Appearance of the tDsRed signals around both the lateral ventricles suggested spread of CPP-fused Cre in the cerebral ventricle. Observation of brain slice from the brain posterior (D) also showed expression of tDsRed in Cre-L17ER4-treated mice (E).

Conclusion

In this study, the ability of L17E and its arginine-modified derivatives for intracellular delivery of peptides and proteins was evaluated. Analysis of the cellular uptake efficiency of fluorescein-labeled peptides (fluorescein can be regarded as a small-molecule model cargo) showed that L17E had a relatively low cell-permeation activity compared with the frequently employed R8. However, notably, arginine modification was effective in improving the cell permeation ability, especially in the case of L17ER4. Intracellular delivery efficacy analyzed by activity-based assays on the delivery of the HiBiT peptide and Cre recombinase suggested the potential ability of L17ER4 as a CPP, especially for intracellular delivery of bioactive peptides. Additionally, the applicability of L17ER4 to *in vivo* protein delivery was also exemplified through gene recombination assay using a Cre-reporter knock-in mouse. Considering that a similar approach of adding arginine residues to ACAL peptides may be applicable to other ACAL and other endosomolytic peptides, this study illustrates a viable approach to designing novel CPPs with unique delivery characteristics.

Acknowledgements

This work was supported by JSPS KAKENHI (Grant Numbers JP20H04707, JP21H04794), and by JST CREST (Grant Number JPMJCR18H5). K.S. and M. A. are grateful for the JSPS Research Fellowship for Young Scientists. T. I. is grateful for SUNBOR SCHOLARSHIP from Suntory Foundation for Life Sciences.

Supplementary material

Table S1 and Figures S1-S3.

References

1. Guillard S, Minter RR, Jackson RH. Engineering therapeutic proteins for cell entry: the natural approach. *Trends Biotechnol.* 2015;33(3): 163-171.
2. Goswami R, Jeon T, Nagaraj H, Zhai S, Rotello VM. Accessing Intracellular Targets through Nanocarrier-Mediated Cytosolic Protein Delivery. *Trends Pharmacol Sci.* 2020;41(10): 743-754.
3. Zhang Y, Røise JJ, Lee K, Li J, Murthy N. Recent developments in intracellular protein delivery. *Curr Opin Biotechnol.* 2018;52: 25-31.
4. Howl J, Jones S. A new biology of cell penetrating peptides. *Peptide Science.* 2021;113(1): e24154.
5. Futaki S, Arafiles JVV, Hirose H. Peptide-assisted Intracellular Delivery of Biomacromolecules. *Chem Lett.* 2020;49(9): 1088-1094.
6. Pei D, Buyanova M. Overcoming Endosomal Entrapment in Drug Delivery. *Bioconjug Chem.* 2019;30(2): 273-283.
7. Brock DJ, Kondow-McConaghy HM, Hager EC, Pellois JP. Endosomal Escape and Cytosolic Penetration of Macromolecules Mediated by Synthetic Delivery Agents. *Bioconjug Chem.* 2019;30(2): 293-304.
8. Brooks H, Lebleu B, Vivès E. Tat peptide-mediated cellular delivery: back to basics. *Adv Drug Deliv Rev.* 2005;57(4): 559-577.
9. Lönn P, Dowdy SF. Cationic PTD/PPP-mediated macromolecular delivery: charging into the cell. *Expert Opin Drug Deliv.* 2015;12(10): 1627-1636.
10. Stanzl EG, Trantow BM, Vargas JR, Wender PA. Fifteen years of cell-penetrating, guanidinium-rich molecular transporters: basic science, research tools, and clinical applications. *Acc Chem Res.* 2013;46(12): 2944-2954.
11. Futaki S, Nakase I. Cell-Surface Interactions on Arginine-Rich Cell-Penetrating Peptides Allow for Multiplex Modes of Internalization. *Acc Chem Res.* 2017;50(10): 2449-2456.
12. Porosk L, Gaidutšik I, Langel Ü. Approaches for the discovery of new cell-penetrating peptides. *Expert Opin Drug Discov.* 2021;16(5): 553-565.
13. Sagan S, Burlina F, Alves ID, Bechara C, Dupont E, Joliot A. Homeoproteins and homeoprotein-derived peptides: going in and out. *Curr Pharm Des.* 2013;19(16): 2851-2862.
14. Nakase I, Takeuchi T, Tanaka G, Futaki S. Methodological and cellular aspects that govern the internalization mechanisms of arginine-rich cell-penetrating peptides. *Adv Drug Deliv Rev.* 2008;60(4-5): 598-607.
15. Kosuge M, Takeuchi T, Nakase I, Jones AT, Futaki S. Cellular internalization and distribution of arginine-rich peptides as a function of extracellular peptide concentration, serum, and plasma membrane associated proteoglycans. *Bioconjug Chem.* 2008;19(3): 656-664.

16. Tünnemann G, Martin RM, Haupt S, Patsch C, Edenhofer F, Cardoso MC. Cargo-dependent mode of uptake and bioavailability of TAT-containing proteins and peptides in living cells. *FASEB J.* 2006;20(11): 1775-1784.
17. Guha S, Ghimire J, Wu E, Wimley WC. Mechanistic Landscape of Membrane-Permeabilizing Peptides. *Chem Rev.* 2019;119(9): 6040-6085.
18. Li W, Nicol F, Szoka FC. GALA: a designed synthetic pH-responsive amphipathic peptide with applications in drug and gene delivery. *Adv Drug Deliv Rev.* 2004;56(7): 967-985.
19. Kyriakides TR, Cheung CY, Murthy N, Bornstein P, Stayton PS, Hoffman AS. pH-sensitive polymers that enhance intracellular drug delivery in vivo. *J Control Release.* 2002;78(1-3): 295-303.
20. Hatakeyama H, Itho E, Akita H, et al. A pH-Sensitive Fusogenic Peptide Facilitates Endosomal Escape and Greatly Enhanced the Gene Silencing of siRNA-Containing Nanoparticles In Vitro and In Vivo. *Mol Ther.* 2009;17: S388-S388.
21. Nakase I, Kobayashi S, Futaki S. Endosome-disruptive peptides for improving cytosolic delivery of bioactive macromolecules. *Biopolymers.* 2010;94(6): 763-770.
22. Akishiba M, Takeuchi T, Kawaguchi Y, et al. Cytosolic antibody delivery by lipid-sensitive endosomolytic peptide. *Nat Chem.* 2017;9(8): 751-761.
23. Akishiba M, Futaki S. Inducible Membrane Permeabilization by Attenuated Lytic Peptides: A New Concept for Accessing Cell Interiors through Ruffled Membranes. *Mol Pharm.* 2019;16(6): 2540-2548.
24. Tamemoto N, Akishiba M, Sakamoto K, Kawano K, Noguchi H, Futaki S. Rational Design Principles of Attenuated Cationic Lytic Peptides for Intracellular Delivery of Biomacromolecules. *Mol Pharm.* 2020;17(6): 2175-2185.
25. Sakamoto K, Akishiba M, Iwata T, et al. Optimizing charge switching in membrane lytic peptides for endosomal release of biomacromolecules. *Angew Chem Int Ed Engl.* 2020; 59(45):19990-19998.
26. Nomura Y, Sakamoto K, Akishiba M, Iwata T, Hirose H, Futaki S. Improved cytosolic delivery of macromolecules through dimerization of attenuated lytic peptides. *Bioorg Med Chem Lett.* 2020;30(17): 127362.
27. Yu H-H, Sakamoto K, Akishiba M, et al. Conversion of cationic amphiphilic lytic peptides to cell-penetration peptides. *Pept Sci.* 2020;112(1): e24144.
28. Sakamoto K, Akishiba M, Iwata T, Arafles JVV, Imanishi M, Futaki S. Use of homoarginine to obtain attenuated cationic membrane lytic peptides. *Bioorg Med Chem Lett.* 2021;40: 127925.
29. Futaki S. Membrane-permeable arginine-rich peptides and the translocation mechanisms. *Adv Drug Deliv Rev.* 2005;57(4): 547-558.

30. El-Sayed A, Futaki S, Harashima H. Delivery of macromolecules using arginine-rich cell-penetrating peptides: ways to overcome endosomal entrapment. *AAPS J.* 2009;11(1): 13-22.
31. Nakase I, Niwa M, Takeuchi T, et al. Cellular uptake of arginine-rich peptides: Roles for macropinocytosis and actin rearrangement. *Mol Ther.* 2004;10(6): 1011-1022.
32. Kawaguchi Y, Takeuchi T, Kuwata K, et al. Syndecan-4 Is a Receptor for Clathrin-Mediated Endocytosis of Arginine-Rich Cell-Penetrating Peptides. *Bioconjug Chem.* 2016;27(4): 1119-1130.
33. Ishiyama M, Miyazono Y, Sasamoto K, Ohkura Y, Ueno K. A highly water-soluble disulfonated tetrazolium salt as a chromogenic indicator for NADH as well as cell viability. *Talanta.* 1997;44(7): 1299-1305.
34. Dixon AS, Schwinn MK, Hall MP, et al. NanoLuc Complementation Reporter Optimized for Accurate Measurement of Protein Interactions in Cells. *ACS Chem Biol.* 2016;11(2): 400-408.
35. Araki K, Araki M, Miyazaki J, Vassalli P. Site-specific recombination of a transgene in fertilized eggs by transient expression of Cre recombinase. *Proc Natl Acad Sci U S A.* 1995;92(1): 160-164.
36. Hasegawa Y, Daitoku Y, Sekiguchi K, et al. Novel ROSA26 Cre-reporter knock-in C57BL/6N mice exhibiting green emission before and red emission after Cre-mediated recombination. *Exp Anim.* 2013;62(4): 295-304.
37. Cafiso DS. Alamethicin: a peptide model for voltage gating and protein-membrane interactions. *Annu Rev Biophys Biomol Struct.* 1994;23: 141-165.
38. Oh-Hashi K, Furuta E, Fujimura K, Hirata Y. Application of a novel HiBiT peptide tag for monitoring ATF4 protein expression in Neuro2a cells. *Biochem Biophys Rep.* 2017;12: 40-45.
39. Sakamoto K, Akishiba M, Iwata T, et al. Optimizing Charge Switching in Membrane Lytic Peptides for Endosomal Release of Biomacromolecules. *Angew Chem Int Ed Engl.* 2020;59(45): 19990-19998.
40. Cohen-Pfeffer JL, Gururangan S, Lester T, et al. Intracerebroventricular Delivery as a Safe, Long-Term Route of Drug Administration. *Pediatr Neurol.* 2017;67: 23-35.